

SUPPLEMENTARY METHODS

YAP Signature Differential Expression Analysis. We examined the RNA-Seq by Expectation Maximization (RSEM) transformed normalized gene expression values for a previously published YAP expression signature (1) in The Cancer Genome Atlas (TCGA)-CHOL primary tumor samples (n=36) and compared them to TCGA adjacent liver samples (n=50) as well as to Genotype-Tissue Expression (GTEx) database normal liver samples (n=110). The data was downloaded from the University of California Santa Cruz's Xenabrowser (2). These samples were uniformly processed together using University of Santa Cruz's TOIL software. Plots were created using ClustVis software (3).

Human immunohistochemical staining (IHC). Tissue sectioning and IHC staining was performed at the Pathology Research Core (Mayo Clinic, Rochester, MN) using the Leica Bond RX stainer (Leica). FFPE tissues were sectioned at 5 microns and IHC staining was performed on-line. Slides for the PD-L1/Keratin 19 and PD-L1/CD68 stain were retrieved for 20 minutes using Epitope Retrieval 2 (EDTA; Leica) and incubated in Protein Block (Dako) for 5 minutes. The PD-L1 primary antibody (rabbit monoclonal, clone E1L3N, 13684, Cell Signaling) was diluted to 1:400 in Background Reducing Diluent (Dako) and incubated for 15 minutes. Post primary and polymer reagents from the Bond Polymer Refine DAB Detection Kit (Leica) were applied and DAB detection used for PD-L1. The second antibody Keratin 19 (mouse monoclonal, clone RCK108, M0888, Dako) or CD68 (clone PGM1, Dako) were diluted to 1:200 in Background Reducing Diluent (Dako) and incubated for 15 minutes. Post primary and polymer reagents from the Bond Polymer Refine AP-Red Detection Kit (Leica) were applied and AP-Red detection used for CK-19 or CD68. Slides were rinsed between steps with 1X Bond Wash Buffer (Leica) and were counterstained for five minutes using Schmidt hematoxylin and molecular biology grade water (1:1 mixture). Slides were removed from the strainer and rinsed in tap water for five

minutes. Slides were dehydrated in increasing concentrations of ethyl alcohol and cleared in 3 changes of xylene prior to permanent coverslipping in xylene-based medium. Images were acquired with Olympus BX 53 microscope at 20x and 40x.

Cell Culture. Mouse CCA cell line SB cells were maintained in DMEM supplemented with 10% FBS, 0.2% primocin and 0.01% insulin under standard conditions. This cell line was isolated from our murine model of YAP-associated CCA and has been described in detail (4). The murine nonmalignant, immortalized cholangiocyte cell line normal mouse cholangiocyte (NMC) was cultured in Eagle's minimum essential medium supplemented with 10% FBS, penicillin (1,000 U/mL), and streptomycin (100 µg/mL) (5). All cell lines underwent *Mycoplasma* contamination test using Mycoalert[™] Mycoplasma Detection Kit (Lonza).

Mice. Eight-week-old male C57BL/6 mice, BL6 SJL mice (CD45.1 allele) or C57BL mice (CD45.2 allele) were purchased from Jackson Laboratories. Six-week-old male and female C57BL/6 *Ccr2*^{-/-} mice were purchased from Charles River Laboratory and bred at Mayo Clinic. C57BL/6 mice *Pd-11*^{-/-} mice (47) were bred at Mayo Clinic.

Isolation of liver, spleen, or tumor-infiltrating immune cells and flow analysis. Upon excision, tumor, liver and spleen were dissociated with gentleMACS[™] Octo Dissociator (Miltenyi) according to the manufacturer's protocol. CD45⁺ cells were isolated by CD45 (TIL) mouse microbeads (Miltenyi). Cells were incubated with Fixable Viability Stain 510 (BD Horizon[™]) for 15 minutes followed by anti-Fc blocking reagent (Miltenyi) for 10 minutes prior to surface staining. Cells were stained, followed by data acquisition on a Miltenyi MACSQuant® Analyzer 10 optical bench flow cytometer. All antibodies were used following the manufacturer recommendation and Fluorescence Minus One controls were used for each independent experiment to establish gates. For subsequent intracellular staining of granzyme B, cells were

stained using the intracellular staining kit (Miltenyi). Analysis was performed using FlowJo™ (TreeStar). Forward scatter (FSC) and side scatter (SSC) were used to exclude cell debris and doublets. The following antibodies were used for flow cytometry staining: F4/80-PE (REA126, Miltenyi), CD11b-PE-Cy5 (M1/70, eBioscience), CD206-PE-Cy7 (C068C2, BioLegend®), CCR2-APC-Vio®770 (REA538, Miltenyi), PD-L1-BV421 (10F.9G2, BioLegend®), F4/80-PE-Vio®770 (REA126, Miltenyi), CD11c-APC (REA754, Miltenyi), Gr-1-APC-Vio®770 (REA810, Miltenyi), Ly6G-PE (Rat 1A8, Miltenyi), Ly6C-APC-Vio®770 (REA796, Miltenyi), CD3-APC-Vio®770 (REA641, Miltenyi), CD8-BV421 (53-6.7, BD Horizon™), CD11a-PE-Vio®770 (REA880, Miltenyi), PD-1-PerCP-Vio®700 (REA802, Miltenyi), granzyme B-PE (REA226, Miltenyi), CD45.1-Vioblue (A20, Miltenyi), CD45.2-PE-Vio®770 (104-2, Miltenyi), 7AAD-annexinV-APC kit (640930, BioLegend®) and Clec4F (MAB2784, R&D System). Clec4F antibody was conjugated with AlexaFluor® 647 antibody labeling kit (Invitrogen®).

Isolation of MDSCs. MDSCs were isolated from tumor tissue using gentleMACS™ Octo Dissociator (Miltenyi) per the manufacturer's protocol. CD45⁺ cells were isolated by CD45 (TIL) mouse microbeads (Miltenyi), stained with Fixable Viability Stain 510 (BD Horizon™), CD11b-PE-Cy5 and Ly6G-PE and immediately separated by cells sorting. MDSCs were sorted as CD11b⁺ Ly6G⁺ on the live cells population.

Isolation of T cells. CD8⁺ T cells were isolated from a single cell suspension of WT mouse spleens. Single cell suspension was filtered through 70µm mesh, centrifuged at 400 g for 10 minutes and re-suspended at 1x10⁸ cell/mL. CD8⁺ T cells were isolated using easy step mouse CD8⁺ T cell isolation kit (#19856, stemcell) per the manufacturer's protocol.

Immunohistochemistry in mouse liver specimens. Liver tissue from euthanized mice was fixed in 4% paraformaldehyde for 48h, embedded in paraffin, and sectioned into 3–5 µm slices.

Paraformaldehyde fixed, paraffin-embedded mouse tumor and adjacent liver sections were deparaffinized, hydrated and incubated with primary antibody overnight at 4°C. Sections were stained with antibody for SOX9 (ab5535; Millipore). Primary antibody was detected with HRP-conjugated secondary antibody and diaminobenzidine (Dako). Liver tissue sections were counterstained with hematoxylin. Images were acquire with a Leica AXIO scope A1 at 10x, 20x and 40x.

Extracellular vesicle (EV) isolation. EVs were isolated from SB cell conditioned medium. SB cell culture was maintained in EV-free culture medium for 24h. The conditioned medium was subsequently collected and EVs were purified by serial ultracentrifugation (2000 RPM for 20 minutes to remove cell debris; 9600 RPM for 20 minutes to remove cell debris; 25500 RPM for 2 hour precipitate EV; 28500 RPM for 2 hour to wash EV with PBS).

BMDM isolation and in vitro culture. BMDM were isolated from the leg of WT or *Pd-l1*^{-/-} mice. Bone marrow was extracted and maintained in a BMDM medium (RPMI 1640 + 10% low endotoxin FBS + L929 condition medium) for 7 days to isolate BMDM. *Pd-l1*^{-/-} BMDM were plated in 6-well plate at 2×10^5 cell and co-cultured with SB cells at a 1:1 ratio for 72h. BMDM were separated by CD45 (TIL) mouse microbeads (Miltenyi), stained with Fixable Viability Stain 510 (BD Horizon™), F4/80-PE and PD-L1-BV421 and analyzed by flow cytometry. For the conditioned medium and EV experiments, BMDM were plated in a 12-well plate at 2×10^5 cell. 24 hours later, BMDM were incubated with 1 mL of SB cell conditioned medium or 1.5×10^{10} particle of SB EVs for 24h. BMDM were separated by CD45 (TIL) mouse microbeads (Miltenyi), stained with Fixable Viability Stain 510 (BD Horizon™), F4/80-PE and PD-L1-BV421 and analyzed by flow cytometry.

Immunoblot Analysis. EVs were purified from SB cells and lysed using RIPA buffer. Proteins were resolved by SDS-PAGE and transferred to nitrocellulose membranes. The following primary antibodies were used for immunoblot analysis: PD-L1 (AF1019, R&D System), CD81 (sc-9158, Santa Cruz) and Alix (2171, Cell Signaling) Membranes were blotted with primary antibody overnight at 4°C at a dilution of 1:500 (PD-L1 and CD81) or 1:1000 (Alix). Proteins were visualized with enhanced chemiluminescence reagents (ECL/ECL Plus, Amersham GE) and Kodak X-OMAT film.

Soluble PD-L1 ELISA. SB cells were plated on a 150mm dish, and once 90%-100% confluence was reached the cell culture medium was changed and collected 24h later. Culture medium was centrifuged at 1,500 RPM for 10 min at 4°C and proteins were concentrated using Amicon Ultra-4 10K. ELISA was performed on SB conditioned medium using DuoSet® Ancillary Reagent Kit 2 (DY008, R&D systems) and Mouse PD-L1/B7-H1, (DY1019-05, R&D systems).

T cell incubation with conditioned medium from murine CCA cells. To neutralize PD-L1 in SB1 conditioned medium, 2 µg/ml anti-PD-L1 antibody (AF1019, R&D) or 2 µg/ml goat IgG isotype (31245, Invitrogen®) was added to the SB conditioned medium before T cell culture. T cells were subsequently isolated from spleen single cell suspension and cultured in SB conditioned medium with PD-L1 neutralized for 24h with CD3/CD28 beads (Gibco Dynabead). T cell INFγ transporters were inhibited 5 hours before flow staining with 5 µg/mL of brefeldin A (1000x) (420601, Biolegend) and Monensin (420701, Biolegend). T cells were stained with Fixable Viability Stain 510, CD3-APC-Vio770, CD4-PerCP-Vio700, CD8-BV421, Ki67-AF700 and INFγ-PE and analyzed by flow cytometry.

Single cell RNA-seq. Whole live cells were washed twice in 1x PBS + 0.04% BSA and immediately submitted to the Mayo Clinic Core for Single Cell sorting (Mayo Clinic, Rochester,

MN). The cells were first counted and measured for viability using either the Vi-Cell XR Cell Viability Analyzer (Beckman-Coulter) or a basic hemocytometer and light microscope. The barcoded Gel Beads were thawed from -80 C and the cDNA master mix was prepared according to the manufacturer's instruction for Chromium Single Cell 3' v3 library kit (10x Genomics). Based on the desired number of cells to be captured for each sample, a volume of live cells was mixed with the cDNA master mix. A per sample concentration of 500,000 cells per milliliter or better is required for the standard targeted cell recovery of 2000 cells. The stock concentration requirements would not change for higher cell recovery numbers. The cell suspension and master mix, thawed Gel Beads and partitioning oil were added to a Chromium Single Cell B chip. The filled chip was loaded into the Chromium Controller, where each sample was processed and the individual cells within the sample were captured into uniquely labeled GEMs (Gel Beads-In-Emulsion). The GEMs were collected from the chip and taken to the bench for reverse transcription, GEM dissolution, and cDNA clean-up. The resulting cDNA contained a pool of uniquely barcoded molecules. A portion of the cleaned and measured pooled cDNA continued on to library construction, where standard Illumina sequencing primers and a unique i7 Sample index were added to each cDNA pool. All cDNA pools and resulting libraries were measured using Qubit High Sensitivity assays (Thermo Fisher Scientific), Agilent Bioanalyzer High Sensitivity chips (Agilent) and Kapa DNA Quantification reagents (Kapa Biosystems). Libraries are sequenced at 60,000 fragment reads per cell following Illumina's standard protocol using the Illumina cBot and HiSeq 3000/4000 PE Cluster Kit. The flow cells are sequenced as 100 X 2 paired end reads on an Illumina HiSeq 4000 using HiSeq 3000/4000 sequencing kit and HCS v3.3.52 collection software. Base-calling is performed using Illumina's RTA version 2.7.3.

Immune electron microscopy. Isolated EV were fixed in 4% paraformaldehyde in 0.1 M phosphate buffer overnight at 4 °C and then placed on a Formvar-carbon-coated grid and air dried for 20 min. After a PBS wash, grids were transferred to 1% glutaraldehyde for 5 minutes and washed with distilled water. The grids were first contrasted with uranyl-oxalate solution and then contrasted and embedded in a mixture of 4% uranyl acetate and 2% methylcellulose (1:9 ratio). The grids were air dried and visualized with a JEOL 1400 electron microscope (JEOL USA, Peabody, MA) at 80 kV. For immunogold staining, grids were fixed as described above and blocked with 10% FBS in PBS for 20 minutes followed by overnight incubation at 4 °C with a primary anti-PD-L1 antibody (R&D system, Minneapolis, MN) in blocking solution. Next, grids were incubated with secondary antibody anti-Goat-12 nm gold or with antibody rabbit anti-goat IgG-Protein A (10 nm) gold (Jackson ImmunoResearch lab, West Grove, PA) for 1h. The grids were contrasted and embedded with a mixture of 4% uranyl acetate and 2% methylcellulose (1:9 ratio), air dried, and subsequently visualized with a JEOL 1400 electron microscope.

Cytokine array. mRNA was extracted from 30 mg of murine tumor tissue using RNeasy plus mini kit (Qiagen). Reverse transcription (RT) was performed using Invitrogen first strand synthesis system (Thermo Fisher Scientific). Real-time polymerase chain reaction (qPCR) was performed using the RT2 Profiler PCR Array (Qiagen) according to the manufacturer's instructions. The threshold cycle (CT) for each well was calculated using the real-time cycler software.

Quantitative Real-Time PCR. RNA was extracted from 20 mg of murine tumor tissue using the RNeasy plus mini kit (Qiagen). RT was performed using the Invitrogen first strand synthesis system (Thermo Fisher Scientific). Real-time PCR (Light Cycler, Roche Diagnostics) for

quantification of the cDNA template was performed using SYBR Green (Roche Diagnostics) as the fluorophore. Target gene expression was calculated using the $\Delta\text{-}\Delta$ CT method. The following primers were used: *Ccl2*, forward primer TTAAAAACCTGGATCGGAACCAA, and reverse primer GCATTAGCTTCAGATTTACGGGT. *Ccl3*, forward primer TTCTCTGTACCATGACACTCTGC, and reverse primer CGTGGAATCTTCCGGCTGTAG. *Ccl4*, forward primer TTCCTGCTGTTTCTCTTACACCT, and reverse primer CTGTCTGCCTCTTTTGGTCAG. *Ccr1*, forward primer CTCATGCAGCATAGGAGGCTT, and reverse primer ACATGGCATCACCAAAAATCCA. *Ccl5*, forward primer GCTGCTTTGCCTACCTCTCC, and reverse primer TCGAGTGACAAACACGACTGC. *Ccr1*, forward primer CTCATGCAGCATAGGAGGCTT, and reverse primer ACATGGCATCACCAAAAATCCA. *Cx3cr1*, forward primer GAGTATGACGATTCTGCTGAGG, and reverse primer CAGACCGAACGTGAAGACGAG. *Cxcl2*, forward primer CATCCAGAGCTTGAGTGTGACG, and reverse primer GGCTTCAGGGTCAAGGCAAACCT. *Cxcl5*, forward primer CCGCTGGCATTCTGTTGCTGT, and reverse primer CAGGGATCACCTCCAAATTAGCG. *Cxcr2*, forward primer TGGCTGGGATTACCTCAAGAACA, and reverse primer TGTGGCTATGACTTCGGTTTGGGT. *Gapdh*, forward primer CCACCCCAGCAAGGAGACT, and reverse primer GAAATTGTGAGGGAGATGCT.

References

1. Yuan WC, Pepe-Mooney B, Galli GG, Dill MT, Huang HT, Hao M, et al. NUA2 is a critical YAP target in liver cancer. *Nat Commun*. 2018;9(1):4834.
2. Goldman MJ, Craft B, Hastie M, Repecka K, McDade F, Kamath A, et al. Visualizing and interpreting cancer genomics data via the Xena platform. *Nat Biotechnol*. 2020.
3. Metsalu T, and Vilo J. ClustVis: a web tool for visualizing clustering of multivariate data using Principal Component Analysis and heatmap. *Nucleic Acids Res*. 2015;43(W1):W566-70.
4. Rizvi S, Fischbach SR, Bronk SF, Hirsova P, Krishnan A, Dhanasekaran R, et al. YAP-associated chromosomal instability and cholangiocarcinoma in mice. *Oncotarget*. 2018;9(5):5892-905.
5. Yahagi K, Ishii M, Kobayashi K, Ueno Y, Mano Y, Niitsuma H, et al. Primary culture of cholangiocytes from normal mouse liver. *In Vitro Cell Dev Biol Anim*. 1998;34(7):512-4.

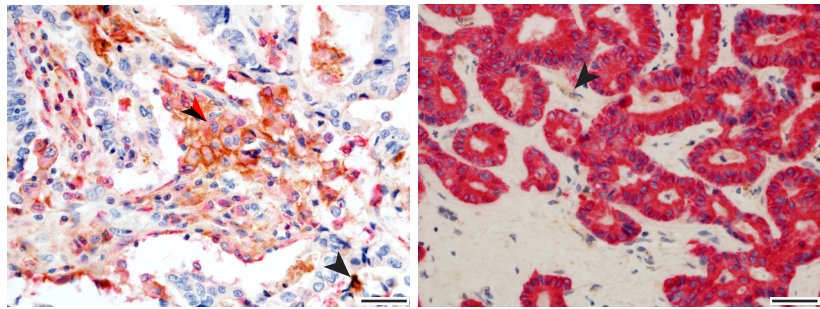
Figure S1

A

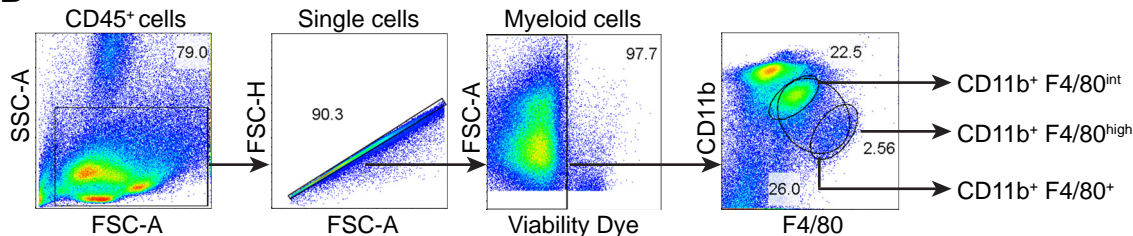
PD-L1/CD68

PD-L1/CK19

Human iCCA

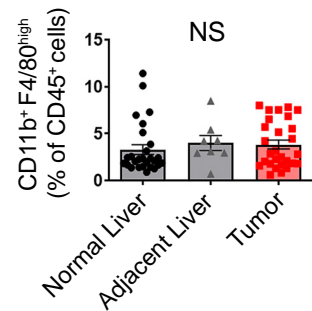


B



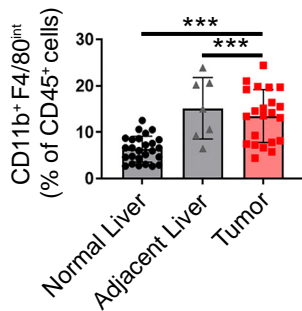
C

F4/80^{high} TAMs



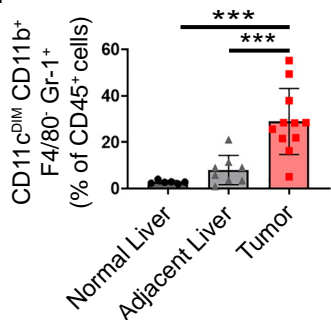
D

F4/80^{int} TAMs



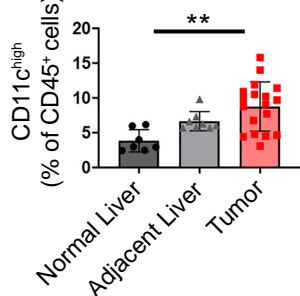
E

MDSCs



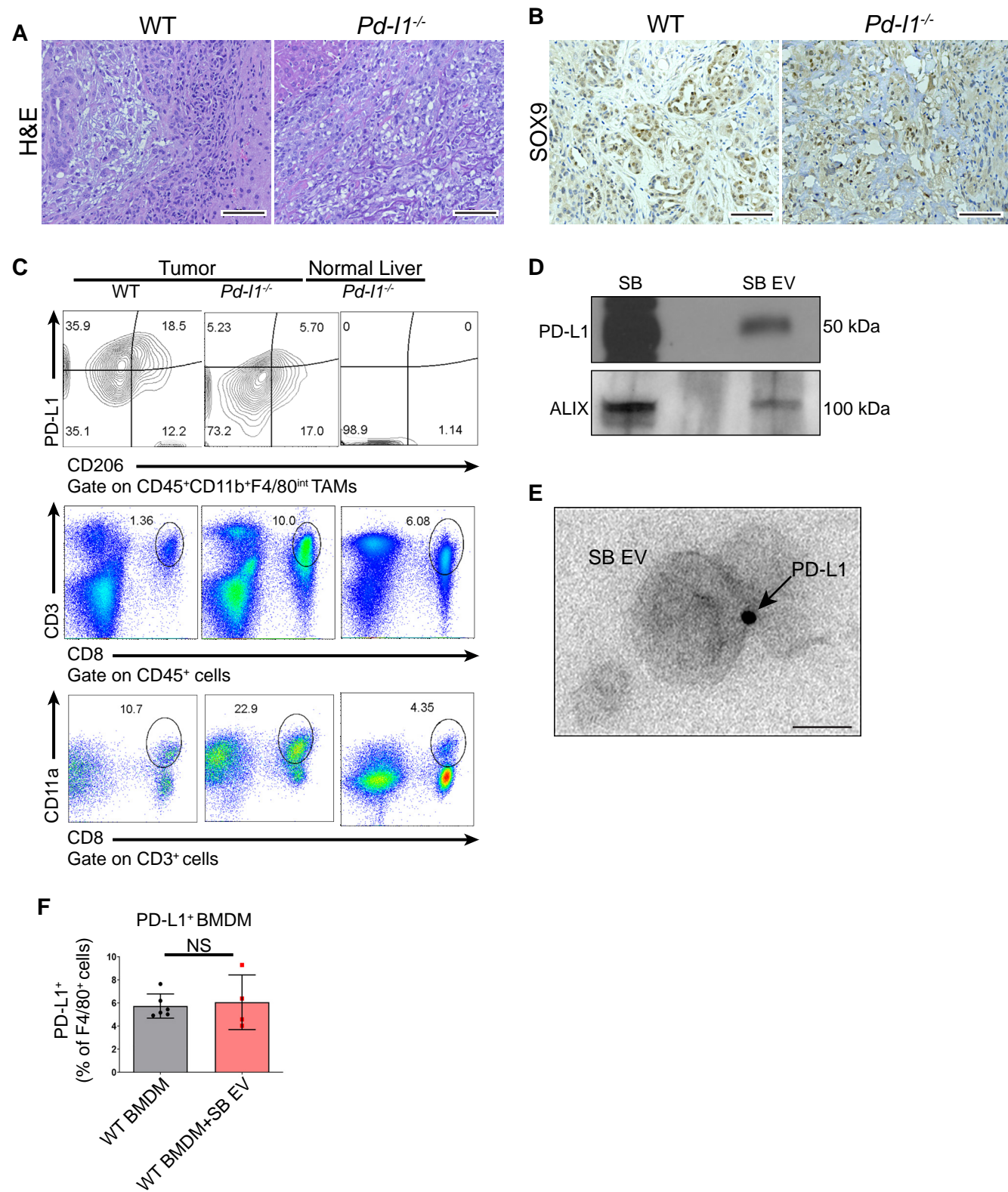
F

Dendritic cells

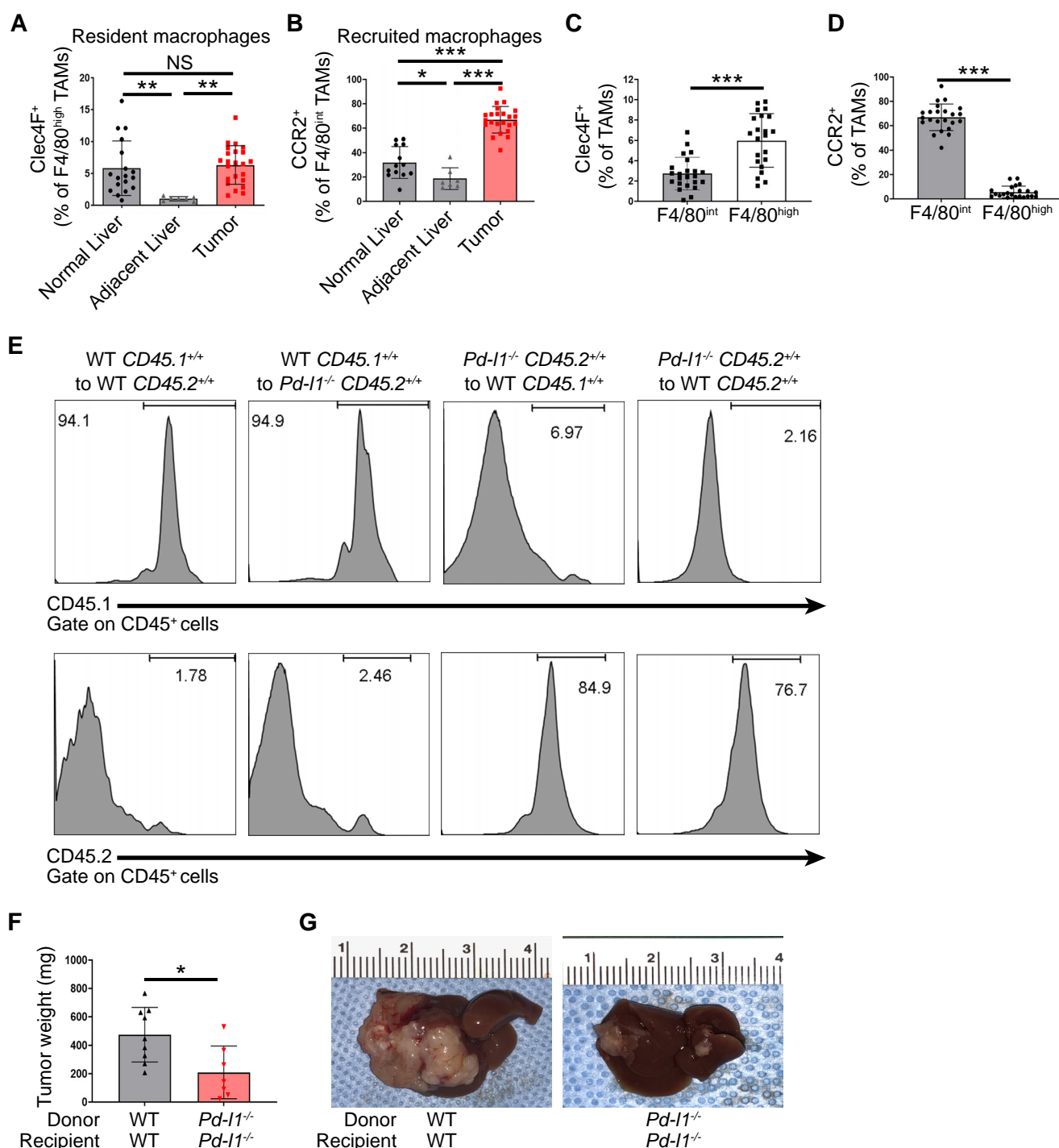


Supplementary Figure S1. TAMs are the predominant source of PD-L1 in CCA. **(A)** Representative images (left and right panels) of PD-L1 (brown staining, black arrow) plus CD68 (red staining, red arrow) co-immunostaining (n=33) and PD-L1 (brown staining) plus cytokeratin-19 (CK-19) (red staining) co-immunostaining (n=18) in human resected CCA specimens. Scale bar, 40 μ m. **(B)** Gating strategy for TAMs is shown in a WT mouse tumor (28 days after orthotopic implantation of 1×10^6 SB cells). **(C-F)** Tumor growth of 28 days after orthotopic implantation of 1×10^6 SB (murine CCA) cells in WT mice. **(C)** Percentage of F4/80^{high} TAMs of total CD45⁺ cells in WT mouse liver (from mice without tumor), tumor adjacent liver or tumor, (n \geq 8). **(D)** Percentage of F4/80^{int} TAMs of total CD45⁺ cells in WT mouse liver, tumor adjacent liver or tumor, (n \geq 7). **(E)** Percentage of CD11c^{Dim}F4/80⁻CD11b⁺Gr-1⁺G-MDSCs of CD45⁺ cells in WT mouse liver, tumor adjacent liver or tumor, (n \geq 6). **(F)** Percentage of CD11c⁺ Dendritic cells of CD45⁺ cells in WT mouse liver, tumor adjacent liver or tumor, (n \geq 6). Data represent mean \pm SD. One-way ANOVA with Bonferroni *post hoc* test (B-E) was used. **, P < 0.01; ***, P < 0.001; NS, non-significant.

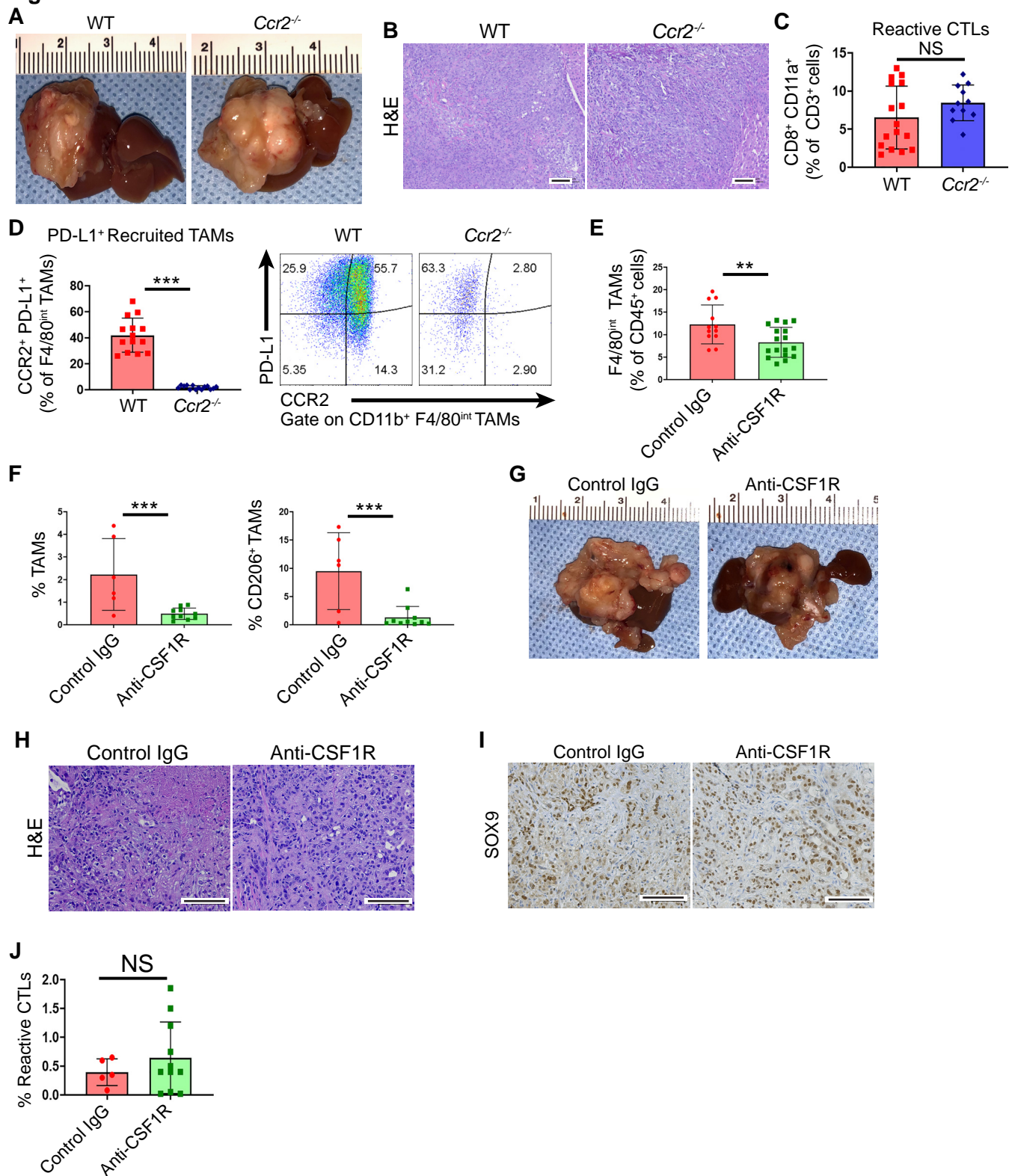
Figure S2



Supplementary Figure S2. Extracellular vesicles do not modulate PD-L1 expression on TAMs. **(A-C)** Tumor growth of 28 days after orthotopic implantation of 1×10^6 SB (murine CCA) cells in WT or *Pd-I1*^{-/-} mouse livers. **(A)** Representative photomicrographs of hematoxylin and eosin-stained SB tumor sections from WT or *Pd-I1*^{-/-} mice. Scale bar, 50 μ m. **(B)** Representative photomicrographs of SOX9 IHC of SB tumor sections from WT or *Pd-I1*^{-/-} mice. Scale bar, 50 μ m. **(C)** Representative flow plots (upper panel) show CD206 and PD-L1 expression of F4/80^{int} TAMs, ($n \geq 8$). Representative flow plots (middle panel) show the population of CD8⁺CD3⁺ CTLs in CD45⁺ cells, ($n \geq 12$). Representative flow plots (lower panel) show the population of CD8⁺CD11a⁺ reactive CTLs of CD45⁺CD3⁺ cells, ($n \geq 12$). **(D)** Immunoblot analysis of PD-L1 in mouse CCA cells (SB cells) and in purified extracellular vesicles (EV) from SB cells. **(E)** Immunogold-labeled PD-L1 in purified EVs from SB cells. **(F)** Percentage of PD-L1⁺F4/80⁺ BMDM after 24h of incubation with 1.5×10^{10} extracellular vesicles from SB cells. BMDM were isolated from WT mice, ($n \geq 4$). Data represent mean \pm SD. Unpaired Student's t test was used. NS, non-significant.

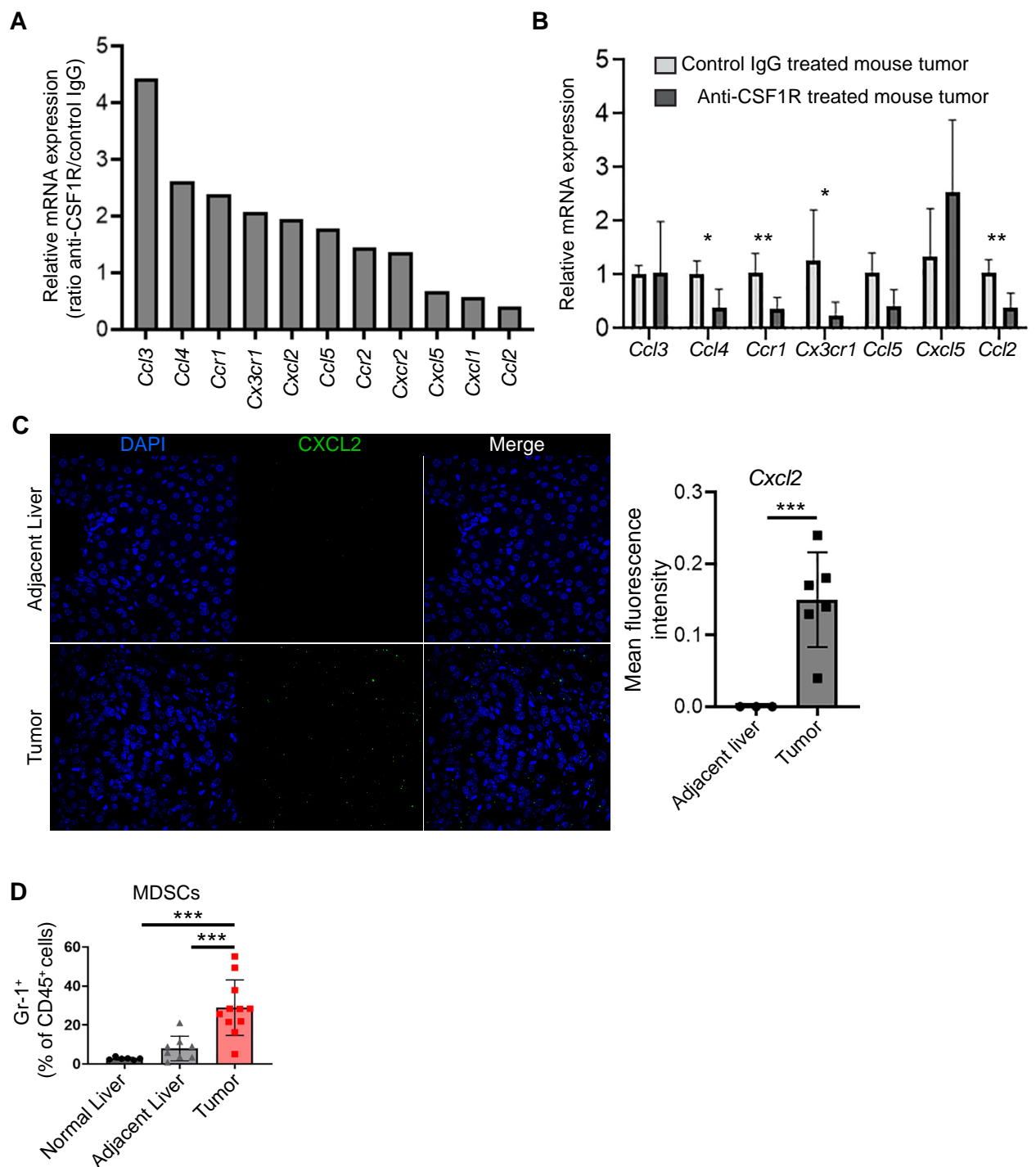
Figure S3

Supplementary Figure S3. PD-L1⁺ TAMs are recruited from the bone marrow in CCA. **(A-G)** Tumor growth of 28 days after orthotopic implantation of 1×10^6 SB (murine CCA) cells in WT mouse livers. **(A)** Percentage of Clec4F⁺ resident TAMs of F4/80^{high} TAMs (CD45⁺CD11b⁺F4/80^{high}) in WT mouse liver, tumor adjacent liver or tumor, ($n \geq 7$). **(B)** Percentage of CCR2⁺ recruited TAMs of F4/80^{int} TAMs (CD45⁺CD11b⁺F4/80^{int}) in WT mouse liver, tumor adjacent liver or tumor, ($n \geq 7$). **(C)** Percentage of Clec4F expression in F4/80^{high} TAMs or F4/80^{int} TAMs (CD45⁺CD11b⁺F4/80⁺) in WT SB tumors, ($n \geq 22$). **(D)** Percentage of CCR2 expression in F4/80^{high} TAMs or F4/80^{int} TAMs (CD45⁺CD11b⁺F4/80⁺) in WT SB tumors, ($n \geq 22$). **(E)** Representative flow histograms show expression of CD45.1, CD45.2, and PD-L1 in CD45⁺ cells after bone marrow transplantation. **(F)** Average tumor weights in milligrams (mg) of WT mice transplanted with WT bone marrow (WT-WT) or Pd-I1^{-/-} mice transplanted with Pd-I1^{-/-} bone marrow (Pd-I1^{-/-}-Pd-I1^{-/-}), ($n \geq 7$). **(G)** Representative pictures of livers from **E**. Data represent mean \pm SD. Unpaired Student's t test (C-D, F) and one-way ANOVA with Bonferroni *post hoc* test (A-B) were used. *, $P < 0.05$; **, $P < 0.01$; ***, $P < 0.001$; NS, non-significant.

Figure S4

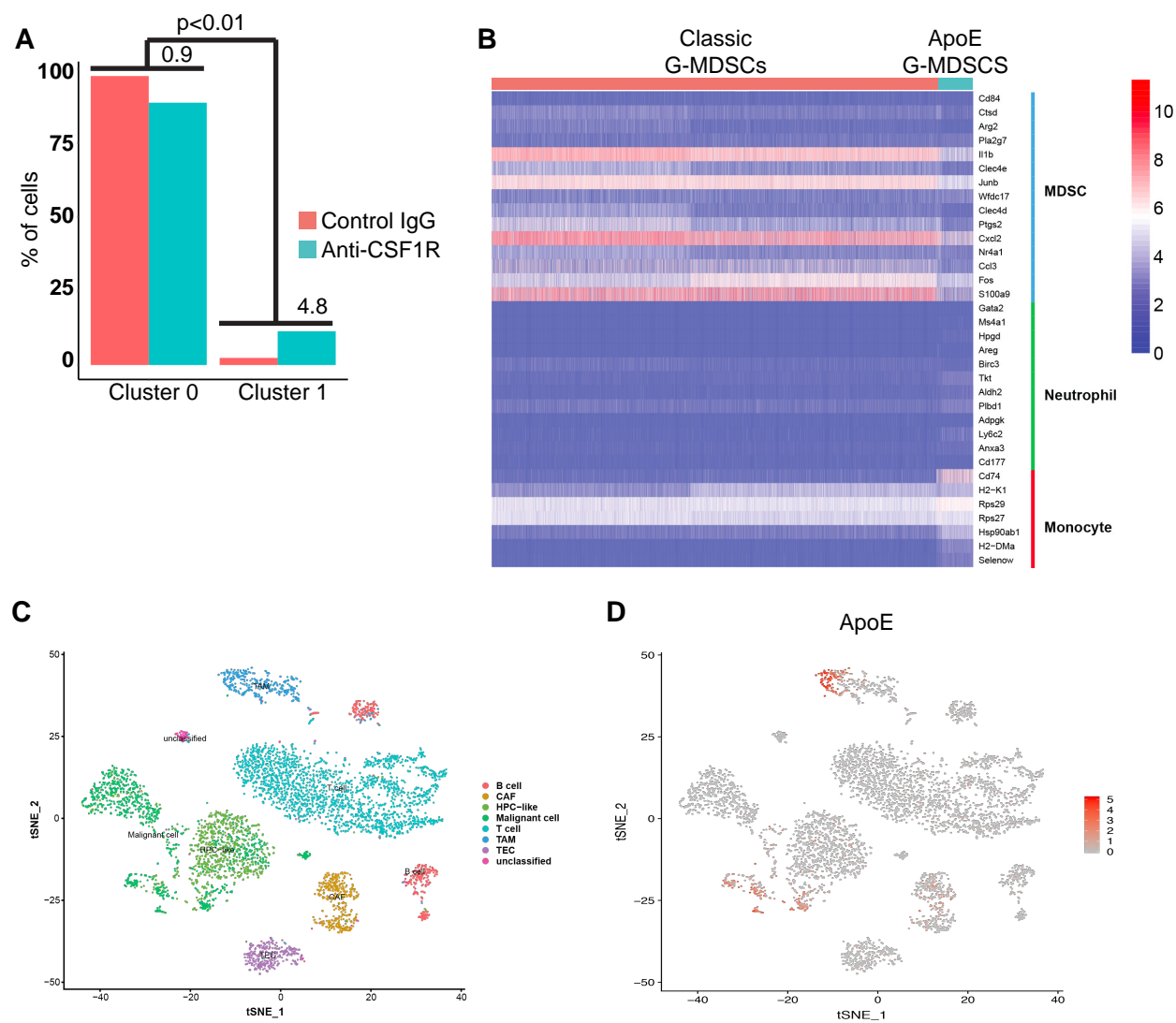
Supplementary Figure S4. TAM blockade does not promote an anti-tumor immune response. **(A-J)** Tumor growth of 28 days after orthotopic implantation of 1×10^6 SB (murine CCA) cells in WT or *Ccr2*^{-/-} mouse livers. **(A)** Representative pictures of livers from WT and *Ccr2*^{-/-} mice. **(B)** Representative photomicrographs of hematoxylin and eosin-stained SB tumor sections from WT or *Ccr2*^{-/-} mice. Scale bar, 50 μ m. **(C)** Percentage of CD8⁺CD11a⁺ reactive CTLs of CD3⁺ cells (CD45⁺CD3⁺) in WT or *Ccr2*^{-/-} tumors, (n=11). **(D)** Percentage of PD-L1⁺CCR2⁺ recruited TAMs of F4/80^{int} TAMs (CD45⁺CD11b⁺F4/80^{int}) in WT or *Ccr2*^{-/-} tumors, (n \geq 11). Representative flow plots show expression of CCR2 and PD-L1 in F4/80^{int} TAMs. **(E)** Percentage of F4/80^{int} TAMs of CD45⁺ cells in SB tumors from WT mice treated with a control Rat IgG isotype or anti-mouse CSF1R, (n \geq 11). **(F)** Percentage of TAMs and CD206⁺ TAMs identified by CyTOF analysis of the markers expressed in CyTOF clusters 19 and 21, respectively, in SB tumors from WT mice treated with a control rat IgG isotype or anti-mouse CSF1R, (n \geq 6). **(G)** Representative pictures of livers from control IgG and anti-CSF1R treated mice. **(H)** Representative photomicrographs of hematoxylin and eosin-stained SB tumor sections from WT mice treated with control Rat IgG isotype or anti-mouse CSF1R. Scale bar, 50 μ m. **(I)** Representative photomicrographs of SOX9 IHC SB tumor sections from WT mice treated with control rat IgG isotype or anti-mouse CSF1R. Scale bar, 50 μ m. **(J)** Percentage of reactive CTLs identified by CyTOF analysis of the markers expressed in cluster 5 in SB tumors from WT mice treated with a control Rat IgG isotype or anti-mouse CSF1R, (n \geq 6). Data represent mean \pm SD. Unpaired Student's t test was used. **, P < 0.01; ***, P < 0.001; NS, non-significant.

Figure S5



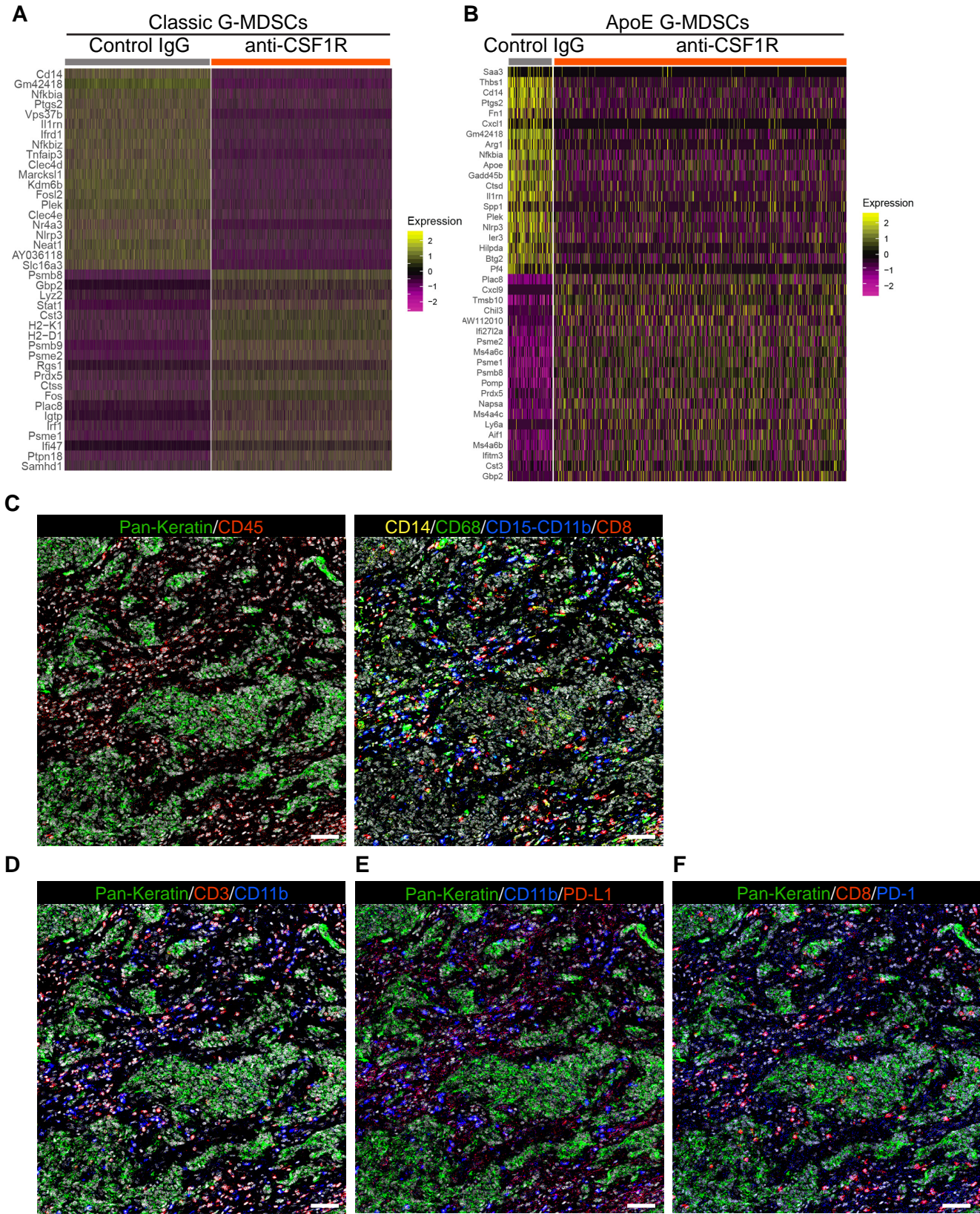
Supplementary Figure S5. CAF-derived CXCL2 is increased in the context of TAM blockade. **(A-D)** Tumor growth of 28 days after orthotopic implantation of 1×10^6 SB (murine CCA) cells in WT mouse livers. **(A)** Ratio of relative mRNA expression of chemokines in anti-CSF1R to control treated tumors (mouse chemokine array). **(B)** Relative mRNA expression of chemokines in control or anti-CSF1R treated SB tumors, ($n \geq 6$). **(C)** Representative immunofluorescence images of *Cxcl2* by *in situ* hybridization in green and nuclei counterstained with DAPI in control or anti-CSF1R treated mouse tumor. Scale bar, 20 μ m. Quantification of mean fluorescence intensity of *Cxcl2* in control or anti-CSF1R treated mouse liver (right panel). **(D)** Percentage of CD11c^{Dim}F4/80⁺CD11b⁺Gr-1⁺MDSCs of CD45⁺ cells in WT mouse normal liver, tumor adjacent liver or tumor, ($n \geq 8$). Data represent mean \pm SD. Unpaired Student's t test (B and C) and one-way ANOVA with Bonferroni *post hoc* test (D) were used. *, $P < 0.05$; **, $P < 0.01$; ***, $P < 0.001$.

Figure S6



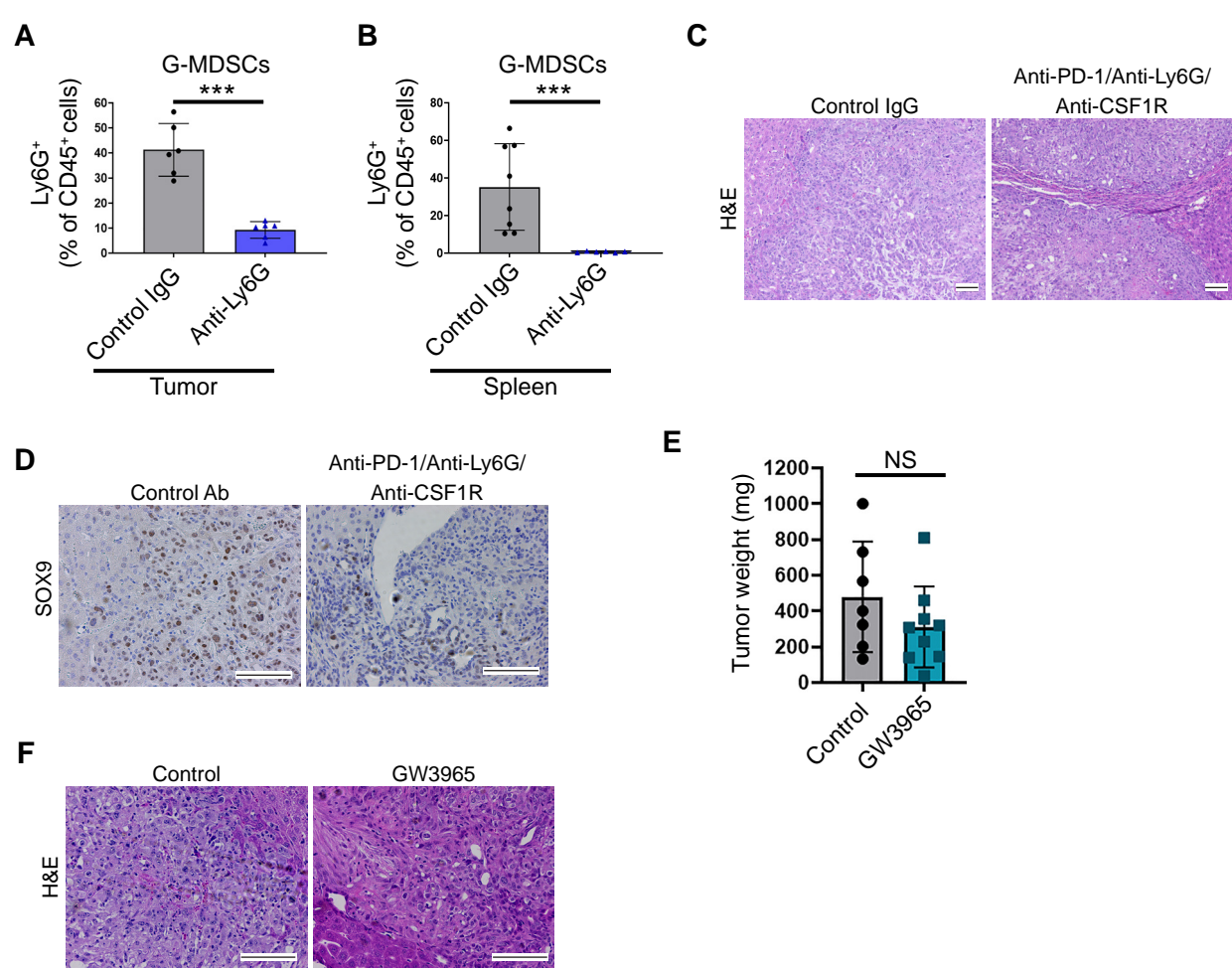
Supplementary Figure S6. Single cell transcriptomics analysis of murine tumors and human CCA scRNA-Seq dataset. **(A-B)** Tumor growth of 28 days after orthotopic implantation of 1×10^6 SB (murine CCA) cells in WT mice. Mice were treated from day 14 to day 28 after implantation with control rat IgG isotype or anti-CSF1R (AFS98). **(A)** Bar plot of percentage of cells in the two clusters for WT mice samples treated with the control IgG or anti-CSF1R. Cell percentage ratio was calculated for each cluster between control and anti-CSF1R group. Fisher's exact test was used to examine the significance. **(B)** Heatmap of expression levels for selective marker genes for MDSCs, neutrophil and monocytes. **(C)** tSNE clustering results for human iCCA data (44). Cells are colored by predicted cell types from the original publication by Ma et al. **(D)** Expression abundance of *ApoE* for human CCA data. Cells with high expression level of *ApoE* are highlighted in red.

Figure S7



Supplementary Figure S7. G-MDSC subsets with survival and immunosuppressive properties. **(A-B)** Tumor growth of 28 days after orthotopic implantation of 1×10^6 SB (murine CCA) cells in WT mice. Mice were treated from day 14 to day 28 after implantation with control rat IgG isotype or anti-CSF1R (AFS98). **(A)** Heatmap of gene expression profiles for top differentially expressed genes between control and anti-CSF1R sample for cells in the Classic G-MDSC subset ($n=20$ for up-regulated genes and $n=20$ for down-regulated genes in treatment sample). Expression values for each gene was z scored across all cells. **(B)** Heatmap of gene expression profiles for top differentially expressed genes between control and anti-CSF1R sample for cells in the ApoE G-MDSC subset ($n=20$ for up-regulated genes and $n=20$ for down-regulated genes in treatment sample). Expression values for each gene was z scored across all cells. **(C-F)** Multiplexed images show various immune cell populations in FFPE tissues from human CCA. Pseudo-colored raw ion images representing the markers of immune cells detected in the region of interest. **(C)** Left panel shows pan-keratin (green), a CCA marker; CD45 (red), a leukocyte marker. Right panel shows CD14 (yellow), a monocyte marker; CD68 (green), a macrophage marker; CD8 (red), a CTL marker; CD11b-CD15 (blue) G-MDSC markers. Scale bar, 100 μ m. **(D)** Pan-keratin (green), a CCA marker; CD3 (red), lymphocyte marker; CD11b (blue), myeloid cell marker. Scale bar, 100 μ m. **(E)** Pan-keratin (green), a CCA marker; CD11b (blue), myeloid cell marker; and PD-L1 (red). Scale bar, 100 μ m. **(F)** Pan-keratin (green), a CCA marker; CD8 (red), a CTL marker; and PD-1 (blue). Scale bar, 100 μ m.

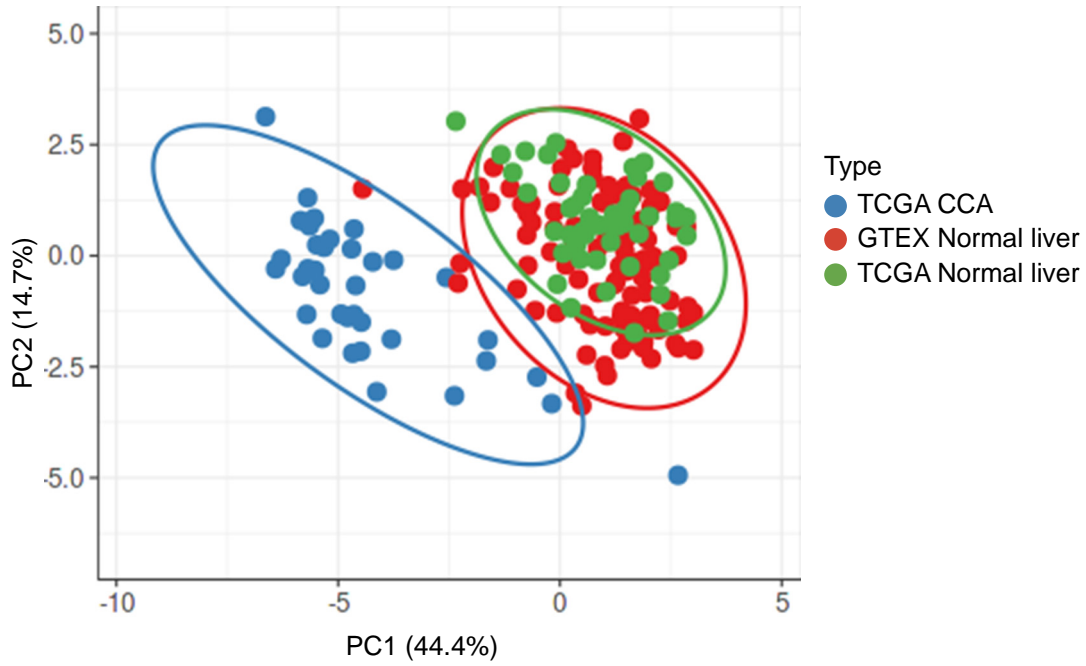
Figure S8



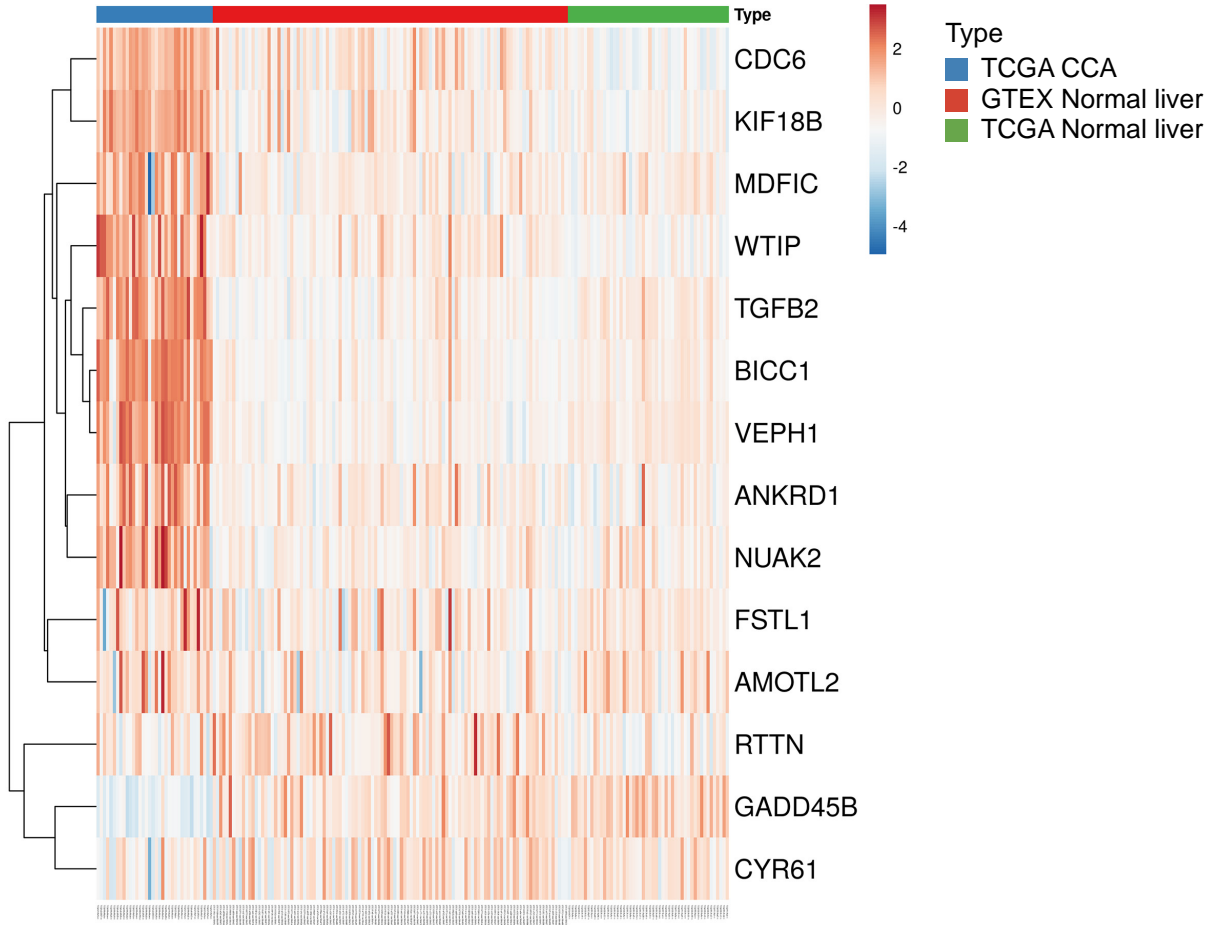
Supplementary Figure S8. Dual inhibition of G-MDSCs and TAMs potentiates anti-PD-1 therapy. **(A-F)** Tumor growth of 28 days after orthotopic implantation of 1×10^6 SB (murine CCA) cells in WT mice. **(A)** Percentage of CD11c^{Dim}F4/80⁻CD11b⁺Ly6G⁺ G-MDSCs of CD45⁺ cells in tumors from WT mice treated with control rat IgG isotype or anti-Ly6G, (n=6). **(B)** Percentage of CD11c^{Dim}F4/80⁻CD11b⁺Ly6G⁺ G-MDSCs of CD45⁺ cells in spleens from WT mice treated with control rat IgG isotype or anti-Ly6G, (n=6). **(C)** Representative photomicrographs of hematoxylin and eosin-stained SB tumor sections from WT mice treated with control IgG isotype or anti-PD-1+anti-CSF1R+anti-Ly6G. Scale bar, 50 μ m. **(D)** Representative photomicrographs of SOX9 IHC of SB tumor sections from WT mice treated with control IgG isotype or anti-PD-1+anti-CSF1R+anti-Ly6G. Scale bar, 50 μ m. **(E)** Average tumor weights in milligrams (mg) of WT mice treated with control IgG isotype or GW3965. **(F)** Representative photomicrographs of hematoxylin and eosin-stained SB tumor sections from WT mice treated with control IgG isotype or GW3965. Scale bar, 50 μ m. Data represent mean \pm SD. Unpaired Student's t test was used. ***, $P < 0.001$; NS, non-significant.

Figure S9

A



B



Supplementary Figure S9. YAP is activated in human CCA. **(A)** Principle component analysis (PCA) comparing YAP signature genes across three cohorts: normal liver samples from Genotype-Tissue Expression (GTEx) database, adjacent liver samples from The Cancer Genome Atlas (TCGA) database, and primary tumor samples from TCGA-CHOL. The expression data being compared are log2 RSEM normalized values. **(B)** Heatmap of the YAP signature genes for normal liver GTEx, adjacent liver TCGA, and primary tumor TCGA-CHOL samples.

TABLES

Supplementary Table S1. Top conserved genes in cluster 0 (Classic G-MDSCs) of murine tumor scRNA-seq dataset.

Gene name	Description	p value	Fold change (Log2)
S100a8	S100 calcium binding protein A8 (calgranulin A)	2.437E-20	1.976
S100a9	S100 calcium binding protein A9 (calgranulin B)	2.571E-18	1.854
Ccl3	chemokine (C-C motif) ligand 3	4.355E-05	1.700
Hcar2	hydroxycarboxylic acid receptor 2	4.398E-15	1.599
Ifitm1	interferon induced transmembrane protein 1	3.996E-13	1.303
Ccr1	chemokine (C-C motif) receptor-like 2	1.290E-09	1.237
Vps37b	vacuolar protein sorting 37B	1.306E-16	1.231
Il1r2	interleukin 1 receptor, type II	1.198E-24	1.172
Hdc	histidine decarboxylase	2.862E-20	1.143
S100a11	S100 calcium binding protein A11	6.871E-21	1.086
Ccr1	chemokine (C-C motif) receptor 1	6.398E-24	1.071
Cxcl2	chemokine (C-X-C motif) ligand 2	7.460E-10	1.065
Msrb1	methionine sulfoxide reductase B1	1.085E-18	1.060
Samsn1	SAM domain, SH3 domain and nuclear localization signals, 1	5.472E-19	1.057
Mxd1	MAX dimerization protein 1	1.704E-15	1.044
Tnfaip2	tumor necrosis factor, alpha-induced protein 2	5.679E-14	1.041
Acod1	aconitate decarboxylase 1	2.566E-06	1.013
Clec4d	C-type lectin domain family 4, member d	3.165E-12	0.976
Stfa211	stefin A2 like 1	2.552E-03	0.968
Pnrc1	proline-rich nuclear receptor coactivator 1	7.669E-20	0.967
Slc7a11	solute carrier family 7, member 11	3.471E-06	0.958
Btg2	B cell translocation gene 2, anti-proliferative	1.211E-22	0.955
Trem1	triggering receptor expressed on myeloid cells 1	5.704E-18	0.951
Srgn	serglycin	8.020E-26	0.947
Clec4e	C-type lectin domain family 4, member e	5.363E-09	0.937
Csf3r	colony stimulating factor 3 receptor (granulocyte)	5.669E-22	0.935
Clec4n	C-type lectin domain family 4, member n	2.106E-13	0.934
Spag9	sperm associated antigen 9	1.517E-18	0.932
Ppp1r15a	protein phosphatase 1, regulatory subunit 15A	5.213E-15	0.919
Il1b	interleukin 1 beta	1.195E-18	0.916

Supplementary Table S2. Top conserved genes in cluster 1 (ApoE G-MDSCs) of murine tumor scRNA-seq dataset.

Gene name	Description	p value	Fold change (Log2)
ApoE	apolipoprotein E	8.754E-121	4.911
Cd74	CD74 antigen	1.103E-42	4.305
H2-Eb1	histocompatibility 2, class II antigen E beta	1.144E-96	3.783
H2-Ab1	histocompatibility 2, class II antigen A, beta 1	3.992E-141	3.771
H2-Aa	histocompatibility 2, class II antigen A, alpha	4.421E-186	3.591
Arg1	arginase, liver	0.000E+00	2.829
S100a4	S100 calcium binding protein A4	1.671E-173	2.470
Tmsb10	thymosin, beta 10	1.524E-77	2.441
Ctss	cathepsin S	1.542E-58	2.279
Psap	prosaposin	8.803E-42	2.239
Lgmn	legumain	6.555E-116	2.112
Npc2	NPC intracellular cholesterol transporter 2	6.319E-73	1.899
Ctsc	cathepsin C	1.240E-108	1.684
Pf4	platelet factor 4	8.876E-221	1.648
Maib	v-maf musculoaponeurotic fibrosarcoma oncogene family, protein B	0.000E+00	1.642
Fcgr2b	Fc receptor, IgG, low affinity IIb	1.009E-137	1.526
Prdx1	peroxiredoxin 1	8.202E-54	1.513
Grn	granulin	4.511E-48	1.422
Fabp5	fatty acid binding protein 5, epidermal	5.831E-13	1.414
Ctsb	cathepsin B	3.282E-25	1.392
Ccr2	chemokine (C-C motif) receptor 2	0.000E+00	1.391
Npm1	nucleophosmin 1	1.464E-59	1.365
Spp1	secreted phosphoprotein 1	4.879E-08	1.353
Tmem176b	transmembrane protein 176B	0.000E+00	1.337
Thbs1	thrombospondin 1	2.883E-24	1.317
Hsp90ab1	heat shock protein 90 alpha (cytosolic), class B member 1	1.546E-36	1.296
Ifi2712a	interferon, alpha-inducible protein 27 like 2A	2.886E-44	1.283
Ly86	lymphocyte antigen 86	0.000E+00	1.277
Ctsh	cathepsin H	1.910E-52	1.259
Aif1	allograft inflammatory factor 1	4.932E-269	1.241
Ccl9	chemokine (C-C motif) ligand 9	4.906E-94	1.211
Trem2	triggering receptor expressed on myeloid cells 2	1.909E-265	1.149

Supplementary Table S3. Human MDSC signature genes.

Human gene name	Description
Ccl2	C-C Motif Chemokine Ligand 2
Ccl5	C-C Motif Chemokine Ligand 5
Ccr2	C-C Motif Chemokine Receptor 2
Cd14	CD14 Antigen
Cd274	Programmed Cell Death 1 Ligand 1
Cd33	CD33 Antigen (Gp67)
Cd34	Hematopoietic Progenitor Cell Antigen CD34
Cd38	CD38 Antigen (P45)
Cd80	CD80 Antigen (CD28 Antigen Ligand 1, B7-1 Antigen)
Csf1	Colony Stimulating Factor 1 (Macrophage)
Csf2	Colony Stimulating Factor 2 (Granulocyte-Macrophage)
Csf3	Colony Stimulating Factor 3 (Granulocyte)
Cxcl1	C-X-C Motif Chemokine Ligand 1
Cxcl12	C-X-C Motif Chemokine Ligand 12
Cxcl2	C-X-C Motif Chemokine Ligand 2
Cxcl5	C-X-C Motif Chemokine Ligand 5
Cxcr2	C-X-C Motif Chemokine Receptor 2
Cxcr4	C-X-C Motif Chemokine Receptor 4
Entpd1	Ectonucleoside Triphosphate Diphosphohydrolase 1
Foxp3	Forkhead Box Protein P3
Ido1	Indoleamine 2,3-Dioxygenase 1
Il10	Interleukin-10
Il1b	Interleukin-1 Beta
Il6	Interleukin-6
Il8	Interleukin-8
Itgam	Integrin, Alpha M (Complement Component 3 Receptor 3 Subunit)
Itgax	Integrin, Alpha X (Complement Component 3 Receptor 4 Subunit)
Nos2	Nitric Oxide Synthase 2A (Inducible, Hepatocytes)
Pdcd1	Programmed Cell Death 1
Ptgs2	Prostaglandin-Endoperoxide Synthase 2
Ptpnc	Protein Tyrosine Phosphatase Receptor Type C
S100a8	S100 Calcium Binding Protein A8
S100a9	S100 Calcium Binding Protein A9
Stat1	Signal Transducer And Activator Of Transcription 1
Stat3	Signal Transducer And Activator Of Transcription 3
Stat5a	Signal Transducer And Activator Of Transcription 5A
Tgfb1	Transforming Growth Factor Beta 1
Tlr3	Toll-Like Receptor 3
Tlr4	Toll-Like Receptor 4
Tnf	Tumor Necrosis Factor

Supplementary Table S4. Human equivalent of ApoE G-MDSC signature genes from murine tumor scRNA seq dataset.

Mouse gene name	Human gene name	Description
Aif1	Aif1	allograft inflammatory factor 1
Apoe	Apoe	apolipoprotein E
Arg1	Arg1	arginase, liver
Ccl9	ccl15	chemokine (C-C motif) ligand 9
Ccl6	Ccl23	chemokine (C-C motif) ligand 6
Ccr2	Ccr2	chemokine (C-C motif) receptor 2
Cd74	Cd74	CD74 antigen
Ctsb	Ctsb	cathepsin B
Ctsc	Ctsc	cathepsin C
Ctsh	Ctsh	cathepsin H
Ctss	Ctss	cathepsin S
Cxcl16	Cxcl16	chemokine (C-X-C motif) ligand 16
Emp3	Emp3	epithelial membrane protein 3
Fabp5	Fabp5	fatty acid binding protein 5, epidermal
Fcgr2b	Fcgr2b	Fc receptor, IgG, low affinity IIb
Gm	Gm	granulin
H2-Aa	HLA-DQA1	histocompatibility 2, class II antigen A, alpha
H2-Ab1	HLA-DQB1	histocompatibility 2, class II antigen A, beta 1
H2-Eb1	HLA-DRB5	histocompatibility 2, class II antigen E beta
Hsp90ab1	Hsp90ab1	heat shock protein 90 alpha (cytosolic), class B member 1
Ifi2712a	IFI27	interferon, alpha-inducible protein 27 like 2A
Lgmn	Lgmn	legumain
Ly86	Ly86	lymphocyte antigen 86
Mafb	Mafb	v-maf musculoaponeurotic fibrosarcoma oncogene family, protein B
Msr1	Msr1	macrophage scavenger receptor 1
Npc2	Npc2	NPC intracellular cholesterol transporter 2
Npm1	Npm1	nucleophosmin 1
Pf4	Pf4	platelet factor 4
Pltp	Pltp	phospholipid transfer protein
Prdx1	Prdx1	peroxiredoxin 1
Psap	Psap	prosaposin
Pycard	Pycard	PYD and CARD domain containing
S100a4	S100a4	S100 calcium binding protein A4
Sgk1	Sgk1	serum/glucocorticoid regulated kinase 1
Spp1	Spp1	secreted phosphoprotein 1
Thbs1	Thbs1	thrombospondin 1
Tmem176b	Tmem176b	transmembrane protein 176B
Tmsb10	Tmsb10	thymosin, beta 10
Tpt1	Tpt1	tumor protein, translationally-controlled 1
Trem2	Trem2	triggering receptor expressed on myeloid cells 2

Supplementary Table S5. CyTOF antibody panel for murine CCA tumor immunophenotyping.

No.	Species Reactivity	Label	Target	Clone	Manufacturer
1	Ms	150Nd	I-A/I-E	M5/114.15.2	Biolegend
2	Ms	143Nd	TCRb	H57-597	Fluidigm
3	Ms	144Nd	MHC Class I	28-14-8	Fluidigm
4	Ms	152Sm	CD3e	145-2C11	Fluidigm
5	Ms	161Dy	Ly6G	1A8	Biolegend
6	Ms	164Dy	CX3CR1	SA011F11	Fluidigm
7	Ms	168Er	CD8a	53-6.7	Fluidigm
8	Ms	172Yb	CD11b (Mac-1)	M1/70	Fluidigm
9	Ms	175Lu	Ly6C	HK1.4	Biolegend
10	Ms	089Y	CD45	30-F11	Fluidigm
11	Ms	166Er	CD19	6D5	Fluidigm
12	Ms	142Nd	CD11c	N418	Fluidigm
13	Ms	154Sm	TER-119	TER-119	Fluidigm
14	Ms	156Gd	CCR2	475301	Novus Biologicals
15	Ms	159Tb	F4/80	BM8	Fluidigm
16	Ms	170Er	CD161 (NK1.1)	PK136	Fluidigm
17	Ms	174Yb	CD115/CSF1R	AFS98	Fluidigm
18	Ms	176Yb	CD45R (B220)	RA3-6B2	Fluidigm
19	Ms	141Pr	Lgals3	202213	Fluidigm
20	Ms	151Eu	CD206 (MMR)	C068C2	Biolegend
21	Ms	155Gd	MERTK	108928	R&D Systems
22	Ms	160Gd	CD64	290322	R&D Systems
23	Ms	165Ho	CD14	Sa14-2	Biolegend
24	Ms	149Sm	Tim4	370901	Biolegend

Supplementary Table S6. Hyperion imaging mass cytometry staining panel for human CCA

<i>No.</i>	<i>Target Name</i>	<i>Metal Tag</i>	<i>Clone</i>	<i>Dilution Factor</i>
1	Alpha-SMA	141Pr	1A4	200
2	CD19	142Nd	6OMP31	400
3	Vimentin	143Nd	D21H3	100
4	CD14	144Nd	EPR3653	200
5	CD16	146Nd	EPR16784	100
6	Pan-Keratin	148Nd	C11	200
7	CD11b	149Sm	EPR16784	100
8	CD45	152Sm	2B11	100
9	CD11c	154Sm	Polyclonal	50
10	FoxP3	155Gd	236A/E7	50
11	CD4	156Gd	EPR6855	400
12	CD68	159Tb	KP1	100
13	Vista	160Gb	D1L2G	50
14	CD20**	161Dy	H1	800
15	CD8a	162Dy	C8/144B	100
16	CD45RA	166Er	HI100	100
17	Granzyme B	167Er	EPR20129-217	50
18	Collagen type 1	169Tm	Polyclonal	600
19	CD3	170Er	Polyclonal	100
20	CD45RO	173Yb	UCHL1	50
21	HLA-DR	174Yb	YE2/36 HLK	50
23	PD-1	165Ho	EPR4877 (2)	50
24	PD-L1	150Nd	E1L3N	50
25	CD15	149Sm	W6D3	50